inter.noise
HAMBURG 2016

Amplified catalogue of vibration reduction index formulas for junctions based on numerical simulations

Jordi POBLET-PUIG[1]; Catherine GUIGOU-CARTER[2]
[1]Universitat Politècnica de Catalunya, Spain
[2]Centre Scientifique et Technique du Bâtiment, France

ABSTRACT
The vibration reduction index (Kij) is a key parameter in the prediction of flanking transmissions according to the EN-12354 standard. Formulas for the evaluation of Kij in L, T and X junctions that depend on the mass ratio are available in the Annex E. Junctions of straight elements with different thickness or thin elastic layers are also included. However, other junction types that are important for building industry are not considered: H-shaped junctions, L or T junctions not forming a right angle, asymmetrical T-junctions , X-junctions where only one of the parts is different (thickness or material) from the other three. In the current research, expressions for these non-covered junctions are provided. They are obtained by means of numerical simulations based on the spectral and/or the standard finite element method. Kij is predicted for a large population of junctions, considering usual thicknesses and material combinations. Afterwards, an statistical treatment of the data is done in order to obtain simple but representative formulas that can easily be used in the daily acoustic projects or included in design software without the need of large computations.

Keywords: flanking, vibration, junction, spectral, finite element
I-INCE Classification of Subjects Number(s): 43.2, 51.4, 51.5, 75.3

1. INTRODUCTION

An important part of the sound transmitted between rooms in a building is done through indirect paths. These paths can be multiple which very often make flanking transmissions to be relevant with respect to the direct transmission path (typically airborne transmission through the wall). Flanking transmission must be predicted by means of global models which take into account not only the insulation capacity of individual elements (i.e. walls) but also the interaction between them and the global behaviour of the building.

A common approach in terms of prediction is to use the model proposed in the EN 12354 standard [1], which is based on the first order SEA formulation proposed in [2, 3]. Among other data, it requires to know the vibration reduction index

$$K_{ij} = \overline{D_{\nu,ij}} + 10\log_{10}\left(\frac{\ell_{ij}}{\sqrt{a_i a_j}}\right) \quad \text{with} \quad a_i = \frac{2.2\pi S_i}{cT_i}\sqrt{\frac{f_{ref}}{f}} \tag{1}$$

where $\overline{D_{\nu,ij}}$ is the direction averaged vibration level difference, ℓ_{ij} is the length of the junction, a_i is the equivalent absorption length of the plate i, S_i its surface, c the speed of sound in the air, $f_{ref} = 1000$ Hz is a reference frequency and T_i the reverberation time of the wall i that can be calculated as $T_i = 2.2/\left(\eta_{total} f\right)$ (being η_{total} the total loss factor).

K_{ij} is the parameter that describes how the vibrations pass from one part of the building to another, typically through the junctions. It is a quite variable parameter that depends on the structure dimensions and junction characteristics. Moreover, the proper quantification of the flanking paths highly depends on the value of K_{ij}.

It can be obtained from experimental measurements of junctions in the laboratory [4, 5]. However, it is time consuming, cumbersome and expensive. This is something to be done in a single junction but it is unrealistic to plan an experimental parametric analysis.

[1]email: jordi.poblet@upc.edu
[2]email: catherine.guigou@cstb.fr

As an alternative to experiments, a common way to estimate K_{ij} is by means of the formulas that are available in the Annex E of [1]. They cover: L, T and X homogeneous junctions, some variations including thin elastic layers between the junction parts and junctions of straight elements with different thickness. K_{ij} can be easily obtained by the evaluation of a formula that depends on the mass ratio of the junction

$$M = \log_{10}\left(\frac{m_\perp}{m_i}\right) \tag{2}$$

M is defined for the vibration transmission path from i to j, m_i is the mass per unit surface of element i (i.e. floor) and $m_\perp$ is the mass per unit surface of the orthogonal element (i.e. wall).

Nevertheless, it seems that the formulas were obtained by statistical approximation of a series of in situ measurements on real buildings. On the one hand, this is good in the sense that reality was tested. But on the other hand, to be coherent with the SEA model in [2, 3], the data should represent first order paths. And it is highly probable that in situ measurements included high-order transmission paths. As shown in [6, 7] it is not easy to define an error-free environment to compute or measure the vibration reduction index. In any case, there are evidences that if the prediction formulas in the Annex E [1] are compared with models of the isolated junction based on Finite Elements (FEM [8]), semi-analytical wave approach [9] or spectral elements (SFEM [10]) some differences are found. These differences are important in the following aspects:

- The formulas in the Annex E are frequency-independent and a single value of K_{ij} is provided for the whole frequency range, while it is seen that K_{ij} can be variable with frequency for some of the junctions and some of the transmission paths.

- The predicted values of K_{ij} in junctions with mass ratio different than one are quite different when computed with Annex E or some of the alternative models of the isolated junctions.

For these reasons, recent researches [8–10] are trying to develop updated formulas than can be used to predict K_{ij} with more detail. Three different frequency ranges are defined: *(i)*low, from 50 Hz to 200 Hz; *(ii)*mid, from 250 Hz to 1000 Hz and *(iii)*high, from 1250 Hz to 5000 Hz. A single value of K_{ij} is provided for each frequency zone: low, mid and high. It is calculated as the arithmetic mean of all third-octave band values. In addition, it was proposed in [8] to characterise the junction by means of the PC variable defined as

$$PC = \log_{10}\left(\frac{\Psi}{\chi}\right) \tag{3}$$

with

$$\frac{\Psi}{\chi} = \left(\frac{\rho_\perp}{\rho_i}\right)^{0.25}\left(\frac{t_\perp}{t_i}\right)^{2.5}\left(\frac{E_\perp}{E_i}\right)^{0.75} \tag{4}$$

where ρ is the volumetric density, t the thickness, E the Young module and the subscripts i and $\perp$ refer to the source element and the orthogonal element respectively. The same Poisson's ratio for the whole junction is assumed.

Ψ/χ includes information not only on the junction mass but also on the stiffness. The PC ratio is more adequate in order to characterise the junctions, especially when the vibration transmission is mainly caused by bending waves.

Other junction models using wave-based semi analytical formulations or Statistical Energy Analysis [11, 12] have also recently been developed. They are an example of the current need of obtaining K_{ij} values for the more simple L, X or T-shaped junctions or even for more complex geometries.

The main goal of the current research is to extend the work presented in [10] to other junction types that are important for building industry but are not considered in the Annex E: H-shaped junctions, L or T junctions not forming a right angle, asymmetrical T-junctions , asymmetrical X-junctions.

In the remainder of the document the method and model used is fast overviewed in Section 2, the results for each of the junction typologies mentioned above can be found in Section 3 and the conclusions are exposed in Section 4.

2. METHODOLOGY

The methodology and the numerical model used to study the new junctions is the same as exposed in [10]. The numerical model, based on shell Spectral Finite Elements (SFEM [13, 14]), is an efficient alternative to solve the elastodynamic problem in structures composed of extrusion symmetry shells in the frequency domain. This efficiency is important in order to perform the large number of simulations required for the parametric analysis, in order to derive general design rules and formulas, to cover a wide frequency range and reproduce the statistical/random character of the physical phenomenon. All the results presented here are limited to the case of point force excitation.

The SFEM model deals with finite size junctions. It means that the proper modal behaviour of the junction is reproduced in each frequency range: a more or less random behaviour at low frequencies controlled by particular modes, and almost SEA behaviour at mid frequencies when the modal overlap increases. However, the final result pretend to be independent on the particular dimensions of the junctions (as the formulas in the Annex E are). With this purpose in mind, a group of 27 junction dimensions are always averaged in order to obtain a single result, representative for all of them. The plate dimensions considered are shown in Table 1, according to the sketch and notations in Figs. 1 and 2(f).

Table 1. Geometrical properties of the plates.

Parameter	Symbol	Value
Lengths in extrusion direction	L_y	4.0, 5.0 , 6.0 m
Lengths for the floors (X, T, L and H)	L_x	3.5, 4.5 , 5.5 m
Height for the wall (X, T and H)	L_z	2.5 m

A population of junctions is considered for each typology. This is generated with the material parameters of Table 2, considering: *(i)* homogeneous junctions made of concrete, aerated concrete blocks and calcium silicate blocks; *(ii)* junctions made of concrete floors (i.e. zones 2 and 5 in the H-junction) and other materials in the walls (i.e. zones 1, 3, 4 and 6 in the H-junction): aerated concrete blocks, bricks or dense aggregate blocks. The total damping is composed by the internal damping (η_{int}) plus the boundary losses considered with $\eta_{boundary} = f^{-0.5}$.

The thicknesses of each zone can be 0.1, 0.2 and 0.3 m with a total of 9 possible combinations. Some more specific geometry detail of each junction typology will be specified when presenting the analysis and results. A range of mass ratios according to common junctions found in heavyweight buildings is therefore covered.

Table 2: Material properties (frequency independent) of the parametric analysis. Same materials as [9] have been considered.

Material	ρ_v (kg/m^3)	ν	E (Pa)	η_{int}
Concrete	2200	0.2	$3.05 \cdot 10^{10}$	0.005
Aerated concrete blocks (1)	400	0.2	$1.39 \cdot 10^{9}$	0.0125
Aerated concrete blocks (2)	800	0.2	$2.77 \cdot 10^{9}$	0.0125
Dense aggregate blocks	2000	0.2	$1.97 \cdot 10^{10}$	0.01
Bricks	1750	0.2	$1.22 \cdot 10^{10}$	0.01
Calcium silicate blocks	1800	0.2	$1.08 \cdot 10^{10}$	0.01

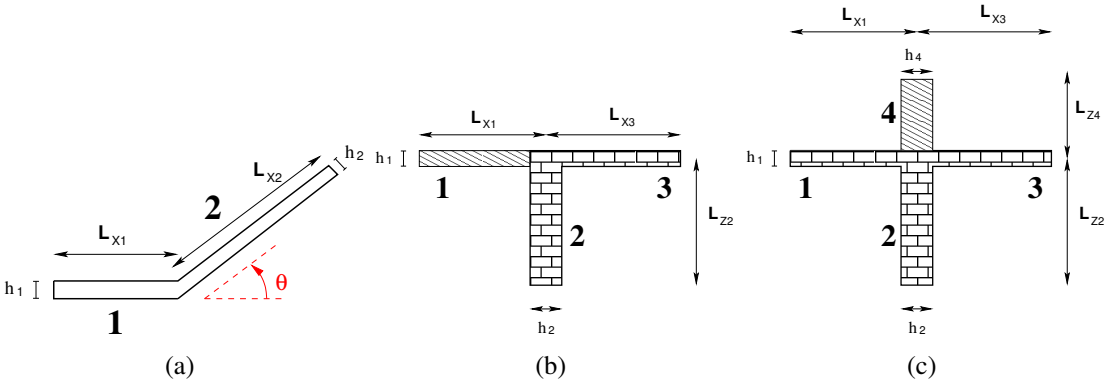

Figure 1: Sketch and notation of the junctions: (a)L-junction with variable angle θ; (b) Asymmetrical T-junction; (c) Asymmetrical X-junction.

3. RESULTS

3.1 H-shaped junctions

Few studies on the vibration reduction index of H-shaped junctions can be found. See [8] that contains K_{ij} expressions for the mid frequency range obtained from FEM simulations and [11, 12] for a detailed model covering several conceptual aspects of the H-junction behaviour.

The sketch of the junction and the notation for of each part is shown in Fig. 2(f). In addition to the comments of Section 2, it must be noted that walls 1, 3, 4 and 6 have always the same material properties and thickness. The same comment is valid for the floors 2 and 5. Four different separations between the internal faces of the walls $3-4$ and $1-6$ are considered: $d = 0.05, 0.1, 0.2$ and 0.3 m.

The K_{ij} of five different paths are computed. The results for the low frequency range are shown in Fig. 2(a-e). The results for the H-junction are compared with the K_{ij} values for the X-junction that were generated by means of a formula [15] that is the best fit to the outputs obtained with the FEM [8], semi-analytical wave approach [9] and SFEM [10].

Fig. 2(a) shows the right-angle transmission between the floor 2 and the first wall 3. No clear trend can be seen for the different wall separations (d). When compared with the X-junction composed of parts 2, 5, 3 and 1, for $\Psi/\chi < 1$ the K_{ij} is larger (taking the X-junction values is on the safe side), while if $\Psi/\chi > 1$ the K_{ij} for the H and the X-junctions is very similar.

Fig. 2(b) shows the right-angle transmission between the floor 2 and the second wall 4. This can be important in order to evaluate the sound transmission between contiguous (left to right) or diagonal (left and bottom to right top) rooms (especially if the separation between walls 3 and 4 is large, long transmission paths are considered, or some floor continuity exist under a double wall). Because the part 4 is the one that radiates sound into the receiving room. In that case, the separation between the leaves of the double wall (d) is relevant and we can see how the data points are more or less ordered from $d = 0.05$ m (the ones with smaller K_{ij}) to $d = 0.3$ m (the ones with larger K_{ij}). In all the cases, the vibration insulation is larger than for an X-junction composed of parts 2, 5, 4 and 6 (with a single wall). This is perfectly logical because the wall 3 represents a barrier for the vibrations that go from part 2 to 4 and vice versa. This effect is more important for the junctions with $\Psi/\chi > 1$ (i.e. with heavier walls 3 and 4). A better lower bound, at least for the zone $\Psi/\chi > 1$, is obtained if an orthogonal wall with double thickness is used in the X-shaped formula ('X low (3+4)').

Fig. 2(c) shows the straight transmission between the floors 2 and 5, in the direction perpendicular to the double wall. Here, there is a clear dependence on the separation between the leaves of the double wall (d). Again it is more important, causing larger variations of K_{ij} for junctions with $\Psi/\chi > 1$. The H-junction results are compared with two different predictions of the X-junction K_{ij}. On the one hand a single X-junction with the floors 2 and 5 and the walls 1 and 3 ('X low (3)'). On the other hand a X-junction where the walls are considered to have double thickness, which is equivalent to put together the leaves $1+6$ and $3+4$ ('X low (3+4)'). All the H-junction results are above either of the single X-junction. The leave separation $d = 0.1$ m is more or less around the double X-junction ('X low (3+4)') while the other H-junction ($d > 0.1$ m) have larger values of K_{ij}.

The K_{ij} values corresponding to the straight transmission between 1 to 3 (or 6 to 4) are shown in Fig. 2(d). Very small differences can be seen between the H-junction (all separations d) and the X-junction. This suggests that using the X-junction formulas is a good approximation for this path.

Finally, the transmission path from 3 to 4 is analysed in Fig. 2(e). The main difference with the path $3-1$ is that now, the separation between the leaves d is important. In addition, the comparison with the single X-junction results is not so good, even for those H-junctions with $d = 0.05$ m.

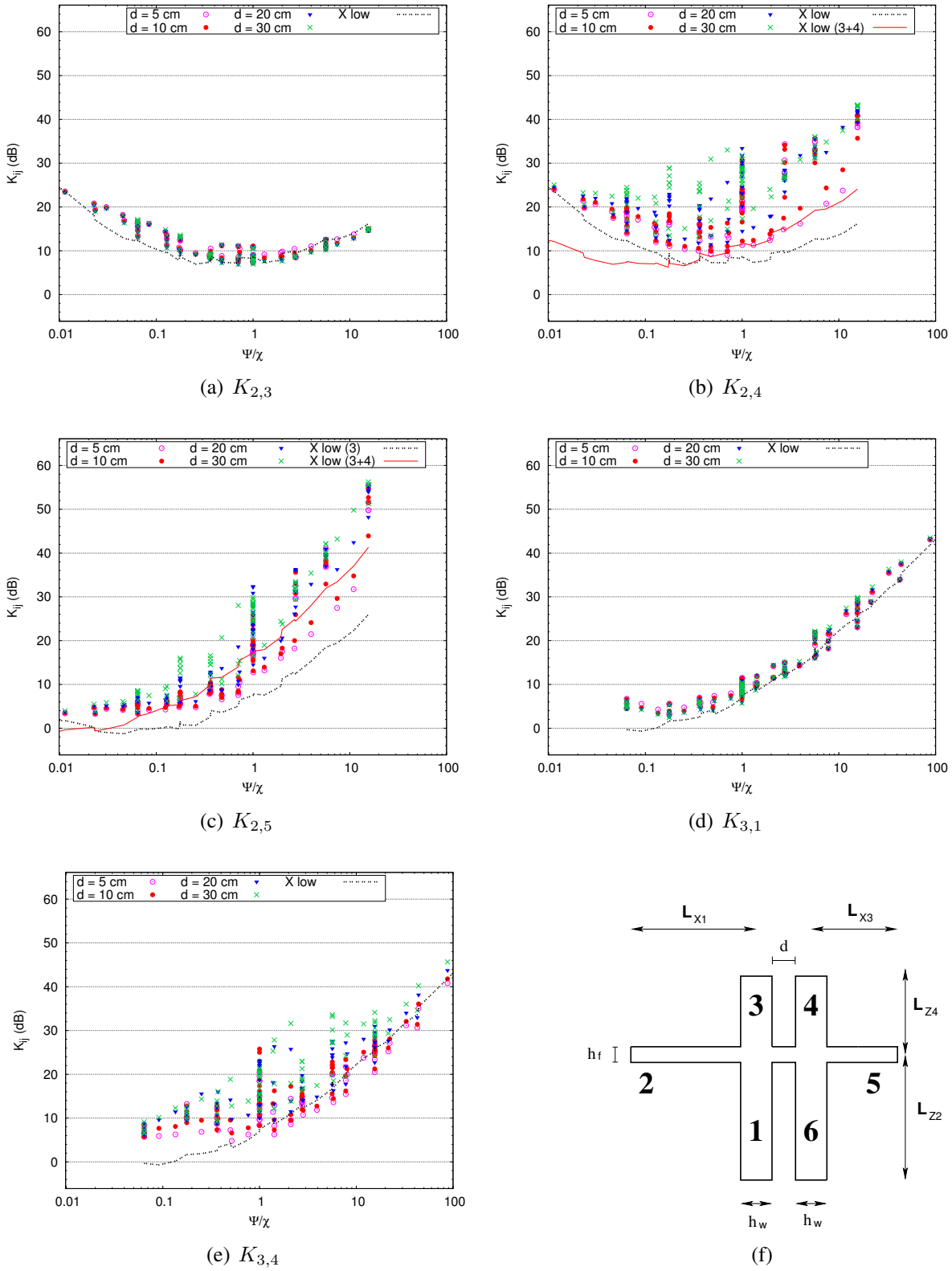

(a) $K_{2,3}$ (b) $K_{2,4}$

(c) $K_{2,5}$ (d) $K_{3,1}$

(e) $K_{3,4}$ (f)

Figure 2: Vibration reduction index K_{ij} for the H-shaped junction in the low-frequency range ($50-200$ Hz): (a-e) several paths; (f) sketch and notation.

3.2 Asymmetrical junctions

The formulas for the T and X junctions in the Annex E as well as in recent researches [8–10] consider only symmetrical junctions. According to the notations in Fig. 1(b) and (c), it means that parts 1 and 3 have always the same thickness and mechanical properties while part 2 can freely vary its properties. In addition, for the X-junction the properties of part 4 must be coincident with the ones in part 2. All these keep the symmetry of the junction and the mass ratio (M) or the Ψ/χ parameter establishes the relationship between orthogonal elements.

However, real buildings can have junctions where this symmetry is lost. This situation is not considered in Annex E and rarely in the literature. A procedure based on the hypothesis that the difference between the sound reduction index of a flanking path and the vibration reduction index is the same for symmetric and for asymmetric junctions was proposed in [16, 17]. This helped in order to obtain K_{ij} curves by means of statistical fitting of many measured flanking paths. A wave based model was formulated in [18] to deal with asymmetrical X-junctions. The model considered bending waves and the transmission loss, taking into account the transmission sense, was computed.

Here it is considered that in the asymmetrical T-junction the thickness and mechanical properties of parts 2 and 3 are the same and independent of part 1 (this is a small simplification because the real asymmetrical junction would have three different properties). In the asymmetrical X-junction only the part 4 will have different properties than the other three parts, that will be made of the same material with equal thickness.

Fig. 3(a) shows the straight transmission $(1-3)$ in such a T-junction. When it is symmetrical, K_{ij} increases if the orthogonal part (2) is heavier or stiffer than the others (1 and 3). Otherwise ($\Psi/\chi < 1$), K_{ij} remains more or less constant. On the contrary, for the asymmetrical T-junction, K_{ij} increases in both situations (large and small Ψ/χ) and has the minimum value around $\Psi/\chi \simeq 1$. Two aspects could explain this behaviour. On the one hand, for $\Psi/\chi > 1$, the heavier orthogonal part of the junction make it difficult to transmit straight vibrations. On the other hand, the different properties of parts 1 and 3 represents an extra difficulty in order to transmit the vibrations between them. And this explains the increase of K_{ij} even for $\Psi/\chi < 1$.

The right-angle transmission between the parts 1 and 2 in the asymmetrical T-junction, see Fig. 3(b), seems to suffer only a shifting in the negative direction of the Ψ/χ parameter. This implies that K_{ij} is larger in the zone where $\Psi/\chi > 1$ and smaller in the zone where $\Psi/\chi < 1$. The minimum value is located around $\Psi/\chi = 0.5$.

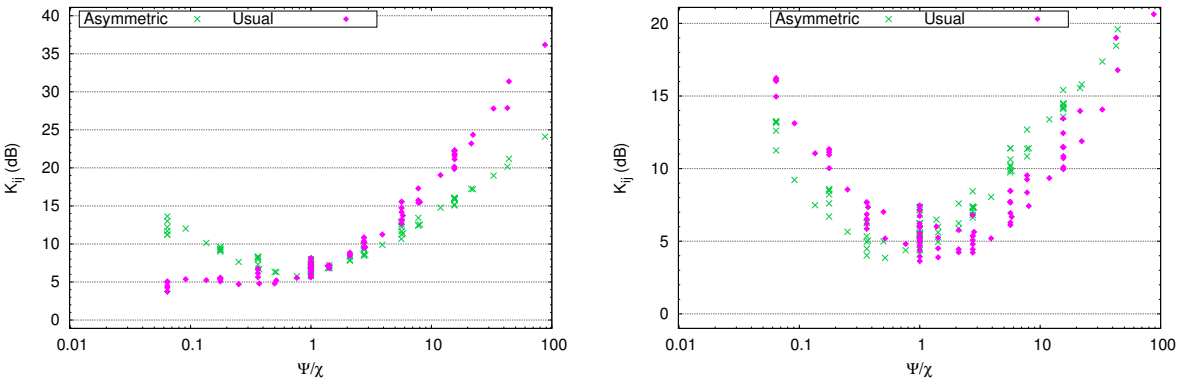

(a) (b)

Figure 3: Comparison of the vibration reduction index K_{ij} for the usual and asymmetrical T-junction in the low-frequency range ($50-200$ Hz): (a) Straight transmission (b) Right-angle transmission $(1-2)$.

The right-angle transmission from 1 to 4 in the the X-junction, see Fig. 4(b), has a very similar behaviour to the T-junction (Fig. 3(b)). The comments for the T-junction are still valid here.

The other path studied here for the X-junction is the straight transmission $1-3$. It is conceptually different to the $1-3$ path in the asymmetrical T-junction because there is no thickness or material change in the transmission direction but only in one of the perpendicular elements. Consequently the general trend of the results differs from the asymmetrical T-junction but is quite similar to the usual (symmetrical) X-

junction. The question here is how different it is from the symmetrical X-junction, or which is the effect of the modification of an orthogonal element. The K_{ij} is slightly larger in the zone where $\Psi/\chi < 1$ and slightly smaller in the zone where $\Psi/\chi > 1$. But these values do not suggest that computing M or Ψ/χ with the averaged properties of walls 2 and 4 would lead to a curve that is equivalent to the symmetrical X-junction one.

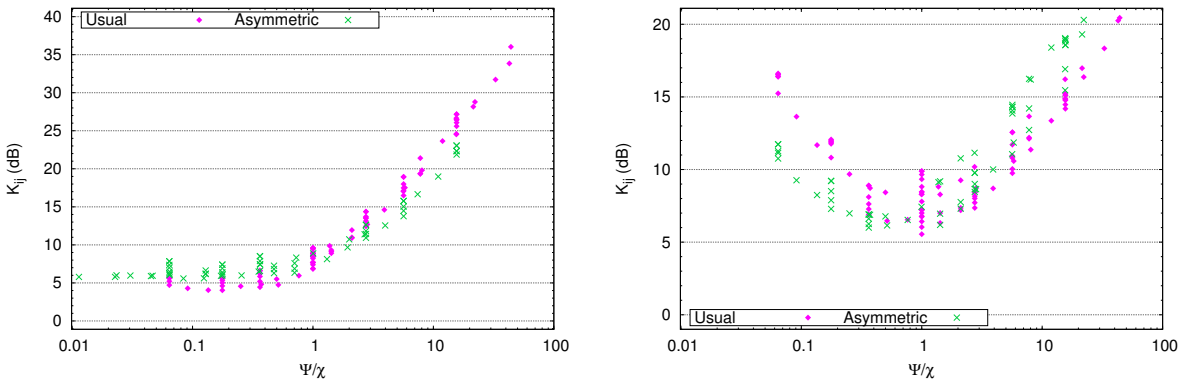

Figure 4: Comparison of the vibration reduction index K_{ij} for the usual and asymmetrical a X-junction in the low-frequency range ($50 - 200$ Hz): (a) Straight transmission (b) Right-angle transmission ($1 - 4$).

3.3 Non-orthogonal L-junctions

Finally, the case of L-junctions with non-orthogonal shape is considered. In fact, non-orthogonal junctions of any type (L, T, X, H) are not taken into account in regulations and the mentioned previous researches.

The sketch and notation for the L-junction is shown in Fig. 1(a). Low and mid-frequency ranges are considered now in order to obtain the results of Fig. 5. The main conclusion is that K_{ij} takes the maximum value for the orthogonal (usual) L-junction. And it decreases while the angle θ tends to 0^o or 180^o. The effect of angle variation is more important when Ψ/χ is different than 1 and clearer in the mid frequencies.

The cases with $\theta > 90^o$ are probably difficult to build in real constructions. A junction of that type would be made and behave more like an U-junction (with short middle plate) instead of an L-junction.

This junction is also used to show the influence of the post-process type. And more precisely, the effect of excluding the zone surrounding (1 m around) the point force from the spatial average. The results are compared in Fig. 6 where the new post-process is labelled with the symbol '*'. The modification in the spatial average of the results obtained with point force excitation causes a reduction of the $K_{i,j}$ values in all cases: low and mid frequencies. It is around 1.5 dB. This is explained because the exclusion of the zone around the force application, that includes the near field, diminished the velocity level in the source plate.

4. CONCLUSIONS AND FUTURE DEVELOPMENTS

The vibration reduction index of some 'less studied' junction types has been computed. As done in previous works [10], the used strategy tries to be general enough in order to provide design guidelines. So, a wide typology of materials and dimensions typically used in buildings is covered.

When comparing with the available formulations and results for standard junctions, meaningful differences are found. This makes evident that the studied junctions require an specific formulation that better describe their behaviour.

The research, in the current state, is still incomplete. Several tasks should be performed in order to enrich this amplified catalogue of vibration reduction index for the 'less usual' junctions:

- Extend the simulations and analysis to the mid and high frequencies. In the present document, mainly the low-frequency range is covered. This is probably the most important for a large quantity of buildings typologies. However, flanking transmissions in the mid and high frequencies where the sound

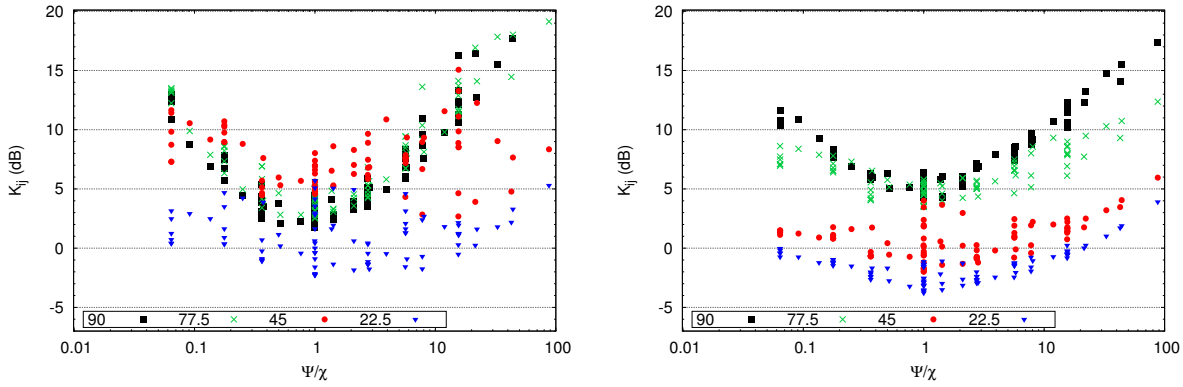

(a) Low, $\theta \leq 90$ (b) Mid, $\theta \leq 90$

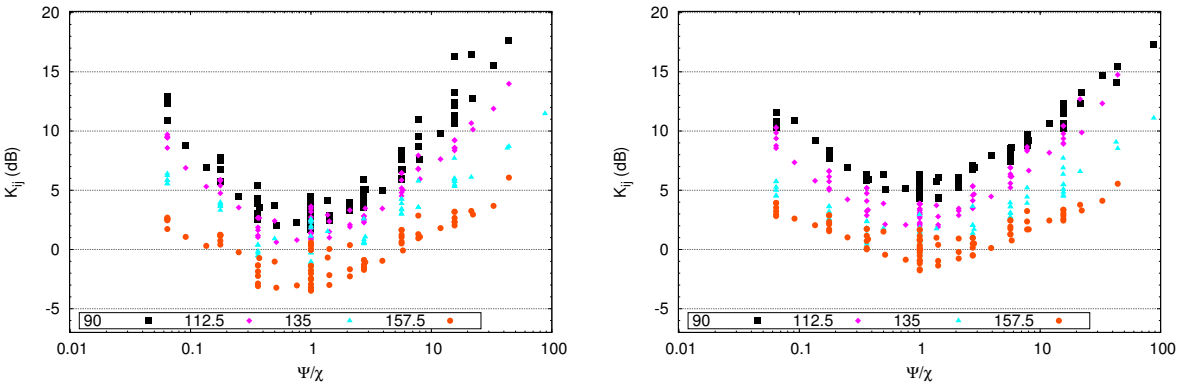

(c) Low, $\theta \geq 90$ (d) Mid, $\theta \geq 90$

Figure 5: Vibration reduction index K_{ij} for the L-shaped junction with different angle θ: (a) and (c) low-frequency range ($50 - 200$ Hz); (b) and (d) mid-frequency range ($250 - 1000$ Hz).

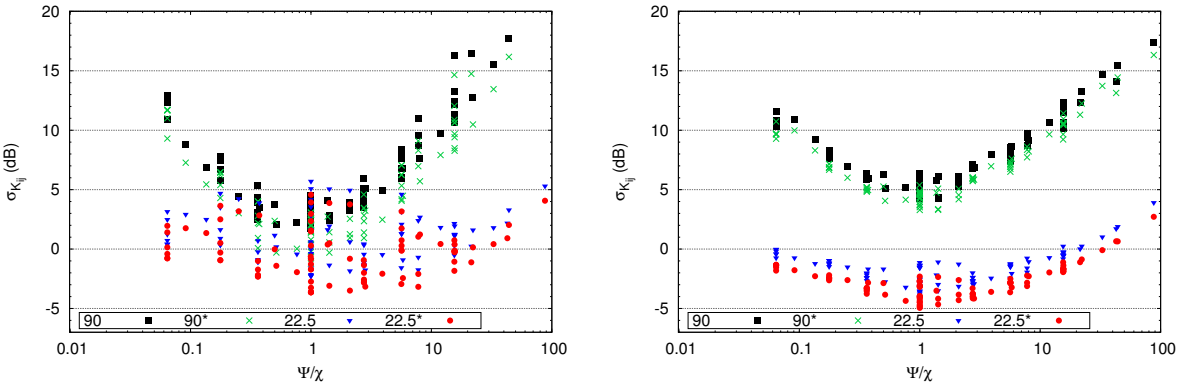

(a) Low (b) Mid

Figure 6: Influence of the post-process of results in the vibration reduction index K_{ij} of the L-shaped junction with different angle θ. '*' means that the zone 1 m around the point force application is excluded from the spatial average: (a) low-frequency range ($50 - 200$ Hz); (b) mid-frequency range ($250 - 1000$ Hz).

reduction index of the direct path is larger can not be systematically neglected in building acoustics designs.

- The results should be synthesized by means of regression equations of the generated data (as done in [8–10]). This is helpful in order to see which are the most important parameters for each junction typology and frequency regime. Moreover if simple expressions are provided, they can be more easily used in acoustic designs.

- Some more understanding on how the different junctions behave would be helpful. This is most

important for the asymmetrical cases.

- Other transmission paths can be analysed for the asymmetrical junctions. For example the transmission $2-3$ in the T-junction or $2-4$ in the X-junction. Also angles between elements in T or X-junctions can be considered.

- Comparison with other modelling techniques would also enrich the research.

ACKNOWLEDGEMENTS

Authors acknowledge financial support from the Research and Development Department of CSTB through Carnot project. Free software has been used [19].

REFERENCES

[1] EN-12354. Building Acoustics: Estimation of the acoustic performance of buildings from the performance of elements. (Acoustique du bâtiment: Calcul de la performance acustique des bâtiments à partir de la performance des éléments). Technical Report 1–4, 1999-2000.

[2] E. Gerretsen. Calculation of the sound transmission between dwellings by partitions and flanking structures. *Appl. Acoust.*, 12(6):413–433, 1979.

[3] E. Gerretsen. Calculation of airborne and impact sound insulation beteen dwellings. *Appl. Acoust.*, 19(4):245–264, 1986.

[4] Ch. Crispin, B. Ingelaere, M. Van Damme, and D. Wuyts. The vibration reduction index K_{ij}: Laboratory measurements for rigid junctions and for junctions with flexible interlayers. *J. Building Acoustics*, 13(2):99–112, 2006.

[5] Ch. Crispin, M. Mertens, B. Blasco, B. Ingelaere, M. Van Damme, and D. Wuyts. The vibration reduction index K_{ij}:laboratory measurements versus predictions EN 12354-1 (2000). In *The 33rd international congress and exposition on noise control engineering*, Prague, 2004.

[6] C. Hopkins. Sound insulation in buildings: linking theory and practice. In *Acoustics 2012*, Nantes, France, 2012.

[7] C. Hopkins and M. Robinson. Using transient and steady-state SEA to assess potential errors in the measurement of structure-borne sound power input from machinery on coupled reception plates. *Applied Acoustics*, 79:35–41, 2014.

[8] Ch. Crispin, L. De Geetere, and B. Ingelaere. Extensions of EN 12354 vibration reduction index expressions by means of FEM calculations. In *Inter-Noise and Noise-con Congress and Conference Proceedings*, volume 249, pages 5859–5868. Institute of Noise Control Engineering, 2014.

[9] C Hopkins. Determination of vibration reduction indices using wave theory for junctions in heavyweight buildings. *Acta Acust. United Acust.*, 100(6):1056–1066, 2014.

[10] J. Poblet-Puig and C. Guigou-Carter. Using spectral finite elements for parametric analysis of the vibration reduction index of heavy junctions oriented to flanking transmissions and EN-12354 prediction method. *Appl. Acoust.*, 99:8–23, 2015.

[11] A. Dijckmans. Structure-borne sound transmission across junctions of finite single and double walls. In *INTER-NOISE and NOISE-CON Congress and Conference Proceedings*, volume 250, pages 2731–2742. Institute of Noise Control Engineering, 2015.

[12] A. Dijckmans. Vibration transmission across junctions of double walls using the wave approach and statistical energy analysis. *Acta Acust. United Acust.*, 102(3):488–502, 2016.

[13] J.F. Doyle. *Wave propagation in structures: spectral analysis using fast discrete fourier transforms*. Springer, New York, 1997.

[14] S. Gopalakrishnan, M. Ruzzene, and S. Hanagud. Spectral finite element method. In *Computational Techniques for Structural Health Monitoring*, pages 177–217. Springer London, 2011.

[15] C. Hopkins, Ch. Crispin, J. Poblet-Puig, and C. Guigou-Carter. Regression curves for vibration transmission across junctions of heavyweight walls and floors based on finite element methods and wave theory. *Submitted*, 2016.

[16] F. Reis. Vibration transmission of asymmetric t form junctions. In *Proceedings of 17th International Congress on Acoustics, Rome*, 2001.

[17] F. Reis. Case studies in predicting airborne sound insulation in building. In *Acustica*, Guimaraes, 2004.

[18] V. J Stauskis and M. Mickaitis. Vibration attenuation at asymmetric cross-form joints of buildings. *Journal of Civil Engineering and Management*, 11(2):129–135, 2005.

[19] C. Geuzaine and J.-F. Remacle. Gmsh: a three-dimensional finite element mesh generator with built-in pre- and post-processing facilities. *Int. J. Numer. Meth. Engng.*, 11(79):1309–1331, 2009.